FASTC-ID(RS)T-0100-93

FOREIGN AEROSPACE SCIENCE AND TECHNOLOGY CENTER

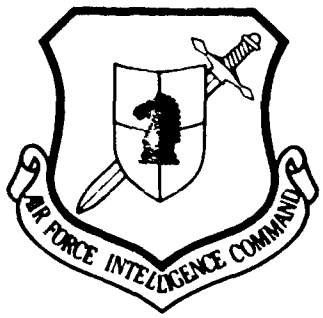

EFFECTS OF STIMULATED RAMAN SCATTERING ON LIGHT BEAM PROPERTIES DURING HIGH-POWER LASER BEAM LONG-PATH PROPAGATION

by

Chien Lian, Shui Zhan, et al.

HUMAN TRANSLATION

FASTC-ID(RS)T-0100-93 3 November 1993

MICROFICHE NR: 93C000626

EFFECTS OF STIMULATED RAMAN SCATTERING ON LIGHT BEAM PROPERTIES DURING HIGH-POWER LASER BEAM LONG-PATH PROPAGATION

By: Chien Lian, Shui Zhan, et al.

English pages: 15

Source: QIONGJIGUANG YU LIZISHU, Vol. 4, No. 2, May 1992; pp. 277-283

Country of origin: China
Translated by: Leo Kanner Associates
F33657-88-D-2188
Requester: FASTC/TATD/Bruce Armstrong

PREPARED BY:

TRANSLATION DIVISION
FOREIGN AEROSPACE SCIENCE AND TECHNOLOGY CENTER
WPAFB, OHIO

GRAPHICS DISCLAIMER

All figures, graphics, tables, equations, etc. merged into this translation were extracted from the best quality copy available.

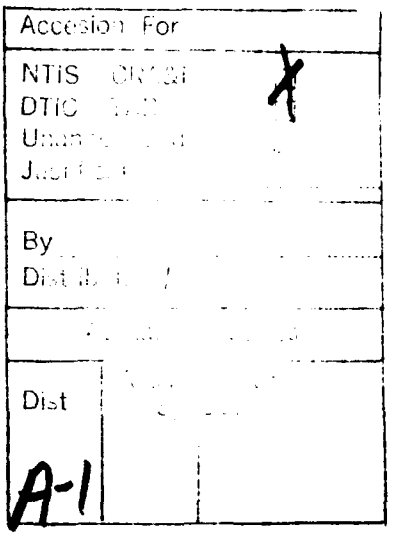

EFFECTS OF STIMULATED RAMAN SCATTERING ON LIGHT BEAM PROPERTIES DURING HIGH-POWER LASER BEAM LONG-PATH PROPAGATION

Chien Lian, Shui Zhan, Zhang Xiaomin,
Wei Xiaofeng, Yuan Xiaodong, Ye Jinxiang,
Man Yongzai, and Peng Hansheng
Southwest Institute of Nuclear Physics and
Chemistry, P.O. Box 515, Chengdu 610003

ABSTRACT: Beginning from the third-order nonlinear polarization from the stimulation and induction of matter based on the semiclassical theory of stimulated Raman scattering (SRS), a theoretical model of coupling between the phase of a pump (transmission) laser beam and the phase of the Stokes beam intensity is established for the case of stimulated Raman scattering during long-path propagation of a high-power laser. The model clearly explains how the SRS effect influences the beam properties of the pump laser, including the physical regime and effective factors of time-domain properties and space-domain properties (light beam quality). The theoretical analysis is in fairly satisfactory agreement with the experimental results. In the experiments, measurements of time-domain properties were taken of the pump laser beam and the Stokes beam after transmission in a situation with various conversion efficiencies

η_s. As shown by the results, under conditions of low-conversion efficiencies, basically the time-domain properties of the pump laser beam are not affected by the SRS effect. But when the conversion efficiency η_s is greater than 5 percent, the pulse duration of the pump laser beam is gradually reduced as η_s is increased.

KEY WORDS: Stimulated Raman scattering, pump laser beam, Stokes beam, far-field divergency angle.

I. Introduction

A physical process of stimulated Raman scattering (SRS) occurs during the long-path transmission of a high-power laser; this process not only consumes energy during laser transmission, but most importantly, the light beam quality of laser transmission (or pumping) will be affected to some extent[1]. Up to the present time, quite a few researchers discussed the physical regime and factors[2] of laser energy consumption during transmission based on the properties of SRS increment[2]. However, no one inquired how SRS affects the light beam during laser transmission. This paper will begin from the general theory of the coupling wave equation of the SRS process by way of analysis of the time-space properties of the SRS process during long-path transmission to study relatively closely and to discuss the theoretical and experimental aspects of how the SRS effect influences the light beam quality and factor of the pump laser.

II. Theory

If we neglect linear absorption in the atmosphere, and assume that high-order and anti-Stokes radiation do not exist in the transmission process, the coupling wave equation of the transmission system under the approximation of slowly changing oscillation amplitude is[3]:

$$\frac{\partial E_p(z',t')}{\partial z'} = \frac{i2\pi\omega_p}{\mu_p c}\chi^{(3)}|E_s|^2 E_p \qquad (1a)$$

$$\frac{\partial E_s(z',t')}{\partial z'} = \frac{i2\pi\omega_s}{\mu_s c}\chi^{(3)}|E_p|^2 E_s \qquad (1b)$$

In the equations, $z'=z$, $t'=t-z/v$.

$$v=c/\mu_0\approx c/\mu_p\approx c/\mu_s$$

$$\chi^{(3)}=\frac{1}{4m}\left(\frac{\partial Q}{\partial q}\right)\frac{N(1-2\bar{n})}{(\omega_0^2-\omega_s^2)+2i\omega_s/T_2}$$

$$\equiv \chi_s'+i\chi_s''+\chi_{NR}^{(3)} \qquad (2)$$

$\chi_{NR}^{(3)}$ is the nonresonant third-order nonlinear polarization rate of the medium. $\chi^{(3)}$ is the third-order nonlinear polarization rate of a Raman medium[3]. In addition, there is $\chi^{(3)}_{NR}\approx 0.1|\chi_s''|_{max}$. Generally, the pump laser beam E_p and the Stokes beam field E_s are compound oscillation amplitude. Therefore, we have the following solutions for Eq. (1):

$$E_p(z',t')=|E_p(z',t')|e^{i\Phi_p}\equiv|E_p|e^{i\Phi_p} \qquad (3a)$$

$$E_s(z',t')=|E_s(z',t')|e^{i\Phi_s}\equiv|E_s|e^{i\Phi_s} \qquad (3b)$$

In the equations, $|E_p|$, $|E_s|$; Φ_p, Φ_s are, respectively, the oscillation amplitude and phase of the pump laser beam and the Stokes beam.

Let us substitute Eq. (3) into Eq. (1), and let the virtual and real portions at both sides of the equal sign be equal to each other, and considering $I_{p,s} = \frac{\mu_{p,s} c}{8\pi} |E_{p,s}|^2$

then we have

$$\begin{cases} \frac{\partial I_p}{\partial z'} = \frac{16\pi^2\omega_p}{\mu_p^2 c^2} \chi_s'' I_s I_p & (4a) \\ \frac{\partial I_s}{\partial z'} = -\frac{16\pi^2\omega_s}{\mu_s^2 c^2} \chi_s'' I_p I_s & (4b) \end{cases}$$

$$\begin{cases} \frac{\partial \Phi_p}{\partial z'} = \frac{16\pi^2\omega_p}{\mu_p^2 c^2} [\chi_s' + \chi_{NR}^{(3)}] I_s & (5a) \\ \frac{\partial \Phi_s}{\partial z'} = \frac{16\pi^2\omega_s}{\mu_s^2 c^2} [\chi_s' + \chi_{NR}^{(3)}] I_p & (5b) \end{cases}$$

In the equations, ω_p and ω_s are, respectively, the frequencies of the pump laser beam and the Stokes beam. From the equation for the Manley-Rowe equation[3]

$$I_p(0,t') + I_s(0,t') = I_p(z',t) + I_s(z',t') \equiv I(t') \qquad (6)$$

as well as Eqs. (4) and (5), for solutions of the phase Φ_p of the pump laser beam during resonant transition and assuming conversion efficiency is not too high, we have

$$\Phi_p(z',t') = \frac{16\pi^2\omega_p}{\mu_p^2 c^2 g_s} \chi_{NR}^{(3)} \frac{I_s(0,t') \exp[g_s I(t') z']}{I_p(0,t')} \qquad (7)$$

g_s is the increment coefficient ($g \approx 2.4 \text{cm/TW}^{[2]}$) of the Stokes beam in the medium. We allow for the fact that, owing to factors of diffraction, turbulent flow, thermal blooming, and small-scale self-focusing[4,5] in the transmission process, the distribution of the pump beam becomes nonuniform. Then from Eq. (7) we know that Φ_p is not only a function of z', but also a function of r' and θ' (under the cylindrical coordinate system). From the near-field distribution plot of the pump beam intensity, the light

intensity distribution can be approximately considered as a super-Gaussian type with certain spatial fluctuations (as shown in Fig. 1b).

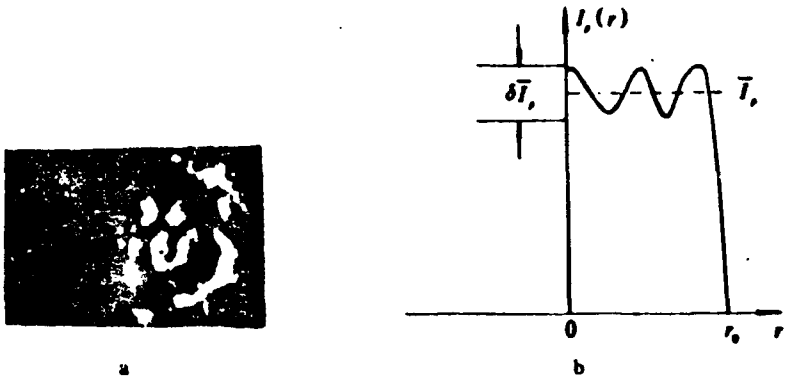

Fig. 1. Diagram of near-field input pump laser beam intensity (a) and its theoretical approximate curve (b)

In the figure, a and b, the light intensity distribution can be described with the following equation:

$$I_p(r)=\bar{I}_p[1+\delta/2\cdot\cos(rm\pi/r_0)] \qquad (8)$$

In the equation, $\delta=(I_{p\max}-I_{p\min})/\bar{I}_p$ is the spatial fluctuation of light intensity; m is the frequency of light intensity fluctuations (generally speaking, m is a positive integer; in the following derivation, m = 2). Substitute Eq. (8) into Eqs. (7) and, based on the Fourier optical principle, we can obtain the relationship between the far-field divergency angle θ_s of the pump laser beam and the limit of the diffraction polarization root of the pump laser beam as such as contributed to by the SRS effect, as given below:

$$\theta_s=\beta[\frac{\exp[\frac{\delta}{2}g_s\bar{I}_p z']}{1+\delta/2}+\frac{\delta g_s\bar{I}_p z'}{\exp(1+g_s\bar{I}_p z')}]\theta_{min} \qquad (9)$$

$$\beta \approx 0.1 \frac{I_s(0,t')\exp(g_s \bar{I}_p z')}{\bar{I}_p}$$

If we neglect the condition of pumping energy consumption, $I_s(0,t')\exp(g_s \bar{I}_p z')/\bar{I}_p$ is the conversion efficiency η_s of the Stokes beam[3]. From Eq. (9), β gradually increases with increase in η_s and in fluctuations δ in the pump laser beam intensity. In the post-transmission pump laser beam, the overall far-field divergency angle $\theta_p = \sqrt{\theta_i^2 + \theta_d^2}$. θ_d is the far-field divergency angle of the pump laser beam before SRS; θ_d is mainly determined by heat distortions of the last-stage spatial filter and rod of the laser apparatus. Under stable experimental conditions, θ_d is a fixed value, that is, $\theta_d \approx 8\theta_{min} = 0.34\text{mrad}$

As mentioned above, only the special effect of ϕ_p is considered. In fact, from Eq. (7) we know that ϕ_p is also a function of t'. Therefore, from the theory of camera station modulation, the frequency spectrum of the pump laser beam field will be broadened[6], that is,

$$\Delta\omega_p = \omega_p - \omega_p^\circ = -\frac{\partial \Phi_p}{\partial t} \qquad (10)$$

ω_p° is the frequency of the pump laser beam before a frequency shift has occurred. Substitute Eq. (7) into Eq. (10) and consider the situation of minor conversion, then we have

$$\Delta\omega_p \approx -\frac{\omega_p^\circ}{\omega_s} \frac{\chi_{NR}^{(3)}}{|\chi_s''|} g_s z' \left(\frac{\partial I_p}{\partial t'} + \frac{\partial I_s}{\partial t'} \right) \frac{I_s^\circ \exp(g_s \bar{I}_p^\circ z')}{\bar{I}^\circ} \qquad (11)$$

I_p^0, I_s^0, I_p, I_s are, respectively, the intensities of the pump laser beam and the Stokes beam, before and after transmission. From Eq. (11) we know that the frequency shift of the post-transmission pump laser beam is related not only to its intensity--time rate of change $\partial I_p/\partial t'$, but also is related to $\partial I_s/\partial t'$ of the Stokes beam.

III. Analysis of Experiments and Results

1. Brief introduction to experimental setup

This experiment was conducted with an LF-11 type Nd:Glass laser device. Fig. 2 shows the optical path diagram of the entire experimental system, and the layout of the instrumentation.

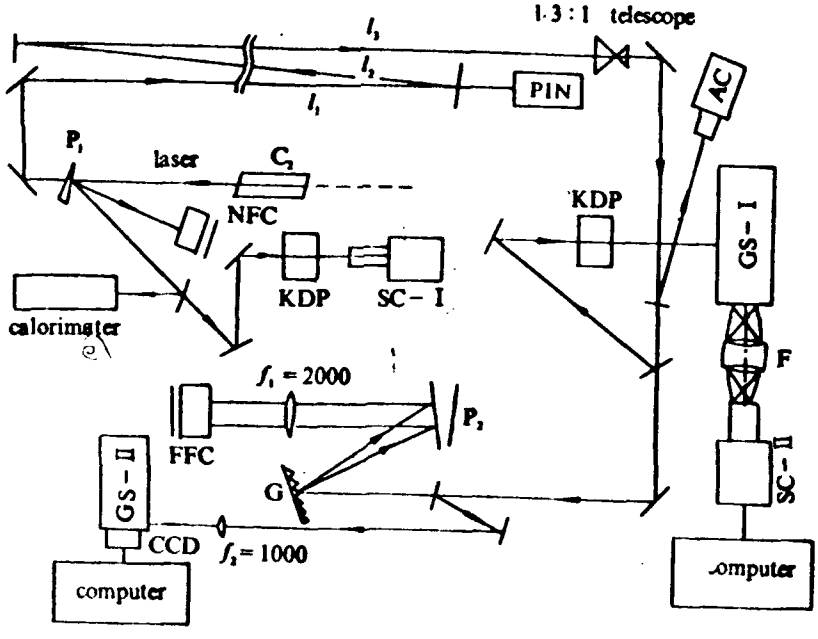

Fig. 2. Optical path of experimental system

KDP: frequency doubling crystal. SC: streak camera. PIN: photodetector. AC: array camera. G: grating. NFC: near-field camera. FFC: far-field camera. GS: grating spectrometer

CCD: CCD camera F: imaging system

The total distance of transmission through air by the pump laser beam outputted from the last-stage amplifier C_2 is $L = I_1 + I_2 + I_3 = 96$ meters. Prior to transmission, the laser parameters (such as, near-field distribution of the quantity of energy, pulse duration, and light intensity) are measured, respectively, with a calorimeter, visible light streak camera SC-I, and near-field camera NFC. The grating spectrograph GS-I and streak camera SC-II are used to measure the time process and interrelationship of the post-transmission pump laser beam and the generated various branches of the Stokes beam (with different wavelengths). The grating G, wedge plate P_2, and the far-field camera FFC are used to measure the far-field divergency angles and the distribution of far-field intensity of the pump laser beam and the various branches of the Stokes beam. The grating spectrograph GS-II and the line array CCD camera are used to measure the post-transmission intensity ratios generated between the various branches of the Stokes beam and the pump laser beam, thus obtaining the Stokes beam conversion efficiency η_s.

2. Results and analysis

During the experiment, the output energy and pulse duration of the laser device are changed so that operations were confined to two situations: in the neighborhood of the SRS threshold (the conversion efficiency is less than or equal to 1 percent of the Stokes beam), and greatly exceeds the threshold value. To ensure actual and reliable experimental results, multiple replications of the experiment were conducted. The results are summarized as

follows:

(1) Influence of the SRS effect on the far-field divergency angle of post-transmission pump laser beam

The spatial distribution of far-field intensity of post-transmission pump laser beam measured with the far-field camera FFC is first scanned with blackness with a CCD camera before computer processing to obtain the far-field divergency angles for conversion efficiency of different kinds of Stokes light (the divergency angle is defined as the divergency angle that corresponds to the size of the focus points accounting for 70 percent of total energy). Fig. 3 shows the variation curves that the far-field divergency angles θ_p of the post-transmission pumping light varies with the conversion efficiency η_s of Stokes light (including the experimental measurement results, and the theoretical calculated results from Eq. (9)). It can be observed that θ_p gradually increases with increase in η_s under our experimental conditions. This observation is consistent with the related theoretical analysis and conclusions in the second part. This conclusion is because distortion occurring at the wave surface of the post-transmission pump laser beam due to Stokes effect and the fluctuations in pump laser beam intensity, thus leading to an increase in the far-field divergency angle.

In addition, by comparing the results of θ_p^{th} and θ_p^{exp}, these two results are in quite good agreement in the case of low conversion efficiency. With an increase in η_s, the difference between the two results gradually grows. This fact is because,

when we used the theoretic model proposed in the paper to compute θ_ρ^{th}, it was considered that the spatial fluctuations were uniform for the intensity of input pumping light (as shown in Eq. (8)); in addition, the model does not strictly consider the instantaneous state factors and the pumping energy consumption brought about by the SRS effect during the pump laser beam transmission. Nonetheless, the authors hold the view that the theoretic model proposed in the paper more successfully explains the physical regime and the destructive factors during the transmission of a high-power laser beam as the SRS effect impairs laser beam quality during transmission.

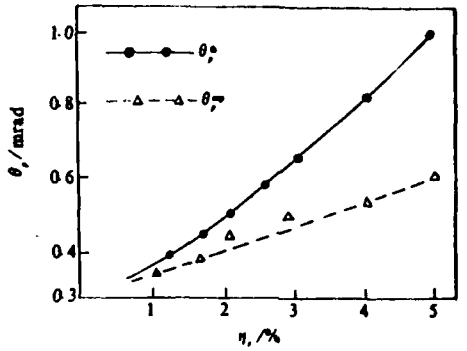

Fig. 3. Variation curves of far-field divergency angle (measured value as θ_ρ^{exp} and calculated value θ_ρ^{th}) of output pump laser with conversion efficiency η_s of Stokes beam

(2) Time-domain properties of output laser beam and Stokes beam under various pumping conditions

When conversion efficiencies of the Stokes beam are, respectively, η_s <, and > 5 percent, the time-domain properties of the transmitted pump laser beam and the Stokes beam (measured

with streak camera SC-II) are, respectively, shown in Figs. 4 and 5. In both figures, a, b, c, and d correspond, in succession, to four situations of η_s in increasing order. The abscissa unit is ch; 1 ch = 5.17 ps. Table 1 shows the corresponding related parameters.

As shown by the data in Fig. 4 and Table 1, the influence on pump laser beam time-domain properties due to SRS is very small when conversion efficiencies are low. The post-transmission pulse shape is still of the Gaussian type, and the variation of pulse duration is very slight in the post-transmission state. As the conversion efficiency η_s increases, the generated peak value of the Stokes beam gradually grows related to the time lag Δt (6) of the pump laser beam peak value. This fact is qualitatively consistent with the numerical calculated results due to Carman et al. in the related instantaneous state conditions[7]. However, here the pulse duration τ_s of Stokes beam also gradually increases. On the other hand, from related data in Fig. 5 and Table 1, the time domain of the post-transmission pump laser beam gradually shortens with increase in the Stokes beam conversion efficiency, when conversion efficiency is high. In addition, the pulse duration of the Stokes beam gradually becomes longer when conversion efficiency is very high. For example, when η_s is approximately 25 percent, the pulse duration of the post-transmission pump laser beam is much shorter. This is due to pumping losses from the SRS effect when conversion efficiency is high.

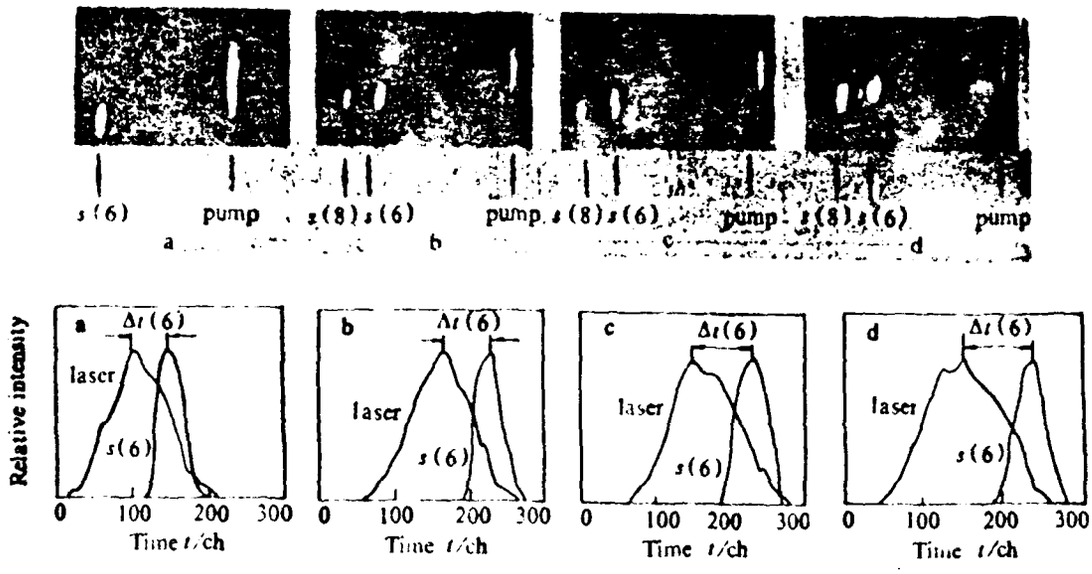

Fig. 4. In the vicinity of the threshold value, time-domain properties (in the diagram, only the time domain of s (6) branches of Stokes beam is plotted; the pump laser beam has attenuated) a, b, c, and d correspond to the conversion efficiencies, in increasing order, for transmitted pump laser beam and Stokes beam

TABLE 1. Pulse Durations (τ_p^o, τ_p) of Pump Laser Beam and Pulse Durations $\tau_s(6)$* of Stokes Beam Before and After Transmission for Different Conversion Efficiencies

	$\eta_s < 5\%$				$\eta_s > 5\%$			
No.	a	b	c	d	a	b	c	d
η_s / %	1.5	2.5	4	5	8	12	15	25
τ_p^o / ps	703	670	740	854	970	950	810	685
τ_p / ps	698	662	734	848	951	905	760	246
$\tau_s(6)$ / ps	259	284	326	352	517	540	624	550

* $\tau_s(6)$ is pulse duration of Stokes beam transited from $J = 6$ to $J = 8$

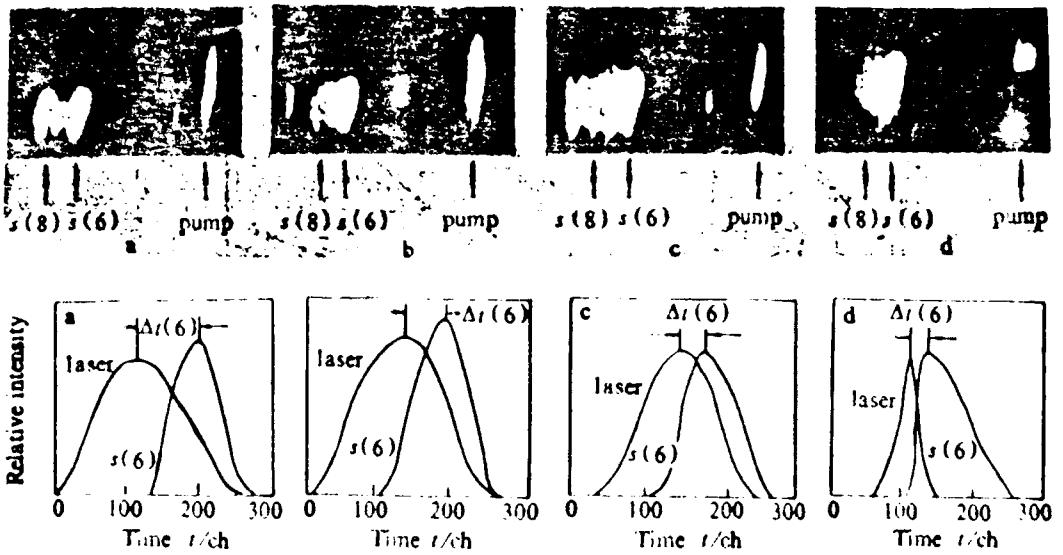

Fig. 5. Time-domain properties (in the figure, only the time domain of s(6) branches of Stokes beam are plotted in the diagram; pump laser beam intensity has attenuated) a, b, c, and d (of the post-transmission pump laser beam and the Stokes beam) correspond to conversion efficiency in increasing order when the conversion efficiency of Stokes beam is high

It is noteworthy that from streak diagrams in Fig. 5, the tail portion of the scanned streaks of the post-transmission pump laser beam has apparent deviation and distortion toward the long-beam direction; in other words, a red shift occurs in the spectral curves. This change is because the results of alternate phase modulation caused by phase coupling of the Stokes beam and the pump laser beam generated during the SRS process. These experimental results are qualitatively consistent with the related conclusions of the theoretical model in the paper, such as that described by Eq. (11).

IV. Conclusions

During the long-path transmission of a high-power laser beam, distortions occur at the waveform surface because of the uneven spatial distribution of stimulated Raman scattering and pump laser beam intensity; thus, the far-field divergency angle of the post-transmission pump laser beam gradually increases as the Stokes beam conversion efficiency increases, and the fluctuations of laser beam intensity become greater. During SRS, the phase of the modulated pump laser beam modulated with Stokes beam intensity leads to a red shift phenomenon in the time domain [two to three characters are missing in the text--Translator] of the pump laser beam. When the pulse duration of the pump laser beam is smaller than 1 ns, as shown in the experimental results, when η_s < 5 percent [three to four characters are missing in the text--Translator], basically the pulse duration and shape of the pump laser beam are not affected by SRS. However, when η_s > 5 percent, the pulse duration of the post-transmission pump laser beam gradually becomes shorter as the Stokes beam conversion efficiency gradually increases.

The authors are grateful to Zhang Jianbo, Tang Can, Liu Hua, Zhao Chunzhuo, and Xie Huaijia et al., for taking part in the work, and Li Wenhong took part in measuring the time-domain properties. The authors benefited greatly in discussions with researchers.

The first draft was received on 21 February 1991; the final revised draft was received for publication on 22 May 1991.

REFERENCES

[1] Henesian MA, Pennington DM. *SPIE*, 1988, **8** (4).
[2] Henesian MA, Murray JR. *Opt Lett*, 1985, **10** : 565.
[3] Penzkofer A, Kaiser W. *Prog Quantum Electron*, 1979, **6**: 66.
[4] Gebhardt FG. *Appl Optics*, 1976, **15**: 1479.
[5] Loy MT, Shen MA. *IEEE J Q E*, 1973, QW-**9**: 409.
[6] ArecchiFT et al. Laser Handbook, North-Holand 1972.
[7] Carman RL, Shimizu F, Wang CS. *Phys Rev*, 1970, A**2**:66.

DISTRIBUTION LIST

DISTRIBUTION DIRECT TO RECIPIENT

ORGANIZATION	MICROFICHE
B085 DIA/RTS-2FI	1
C509 BALLOC509 BALLISTIC RES LAB	1
C510 R&T LABS/AVEADCOM	1
C513 ARRADCOM	1
C535 AVRADCOM/TSARCOM	1
C539 TRASANA	1
Q592 FSTC	4
Q619 MSIC REDSTONE	1
Q008 NTIC	1
Q043 AFMIC-IS	1
E051 HQ USAF/INET	1
E404 AEDC/DOF	1
E408 AFWL	1
E410 ASDIC/IN	1
E411 ASD/FTD/TTIA	1
E429 SD/IND	1
P005 DOE/ISA/DDI	1
P050 CIA/OCR/ADD/SD	2
1051 AFIT/LDE	1
P090 NSA/CDB	1
2206 FSL	1

Microfiche Nbr: FTD93C000626
FTD-1D(RS)T-0100-93